

Thermal Properties of PCL/Gluten Bioblends Characterized by TGA, DSC, SEM, and Infrared-PAS

Abdellatif Mohamed,¹ V. L. Finkenstadt,² Sherald H. Gordon,¹ Girma Biresaw,¹ Palmquist Debra E.,³ P. Rayas-Duarte⁴

¹Cereal Products and Food Science Unit, National Center for Agriculture Utilization Research, USDA-ARS, Peoria, Illinois 61604

²Plant Polymer Research Unit, National Center for Agriculture Utilization Research, USDA-ARS, Peoria, Illinois 61604

³National Center for Agriculture Utilization Research, USDA-ARS, Peoria, Illinois 61604

⁴Food and Agricultural Products Research Center, Oklahoma State University, Stillwater, Oklahoma

Received 3 April 2008; accepted 9 June 2008

DOI 10.1002/app.28914

Published online 10 September 2008 in Wiley InterScience (www.interscience.wiley.com).

ABSTRACT: Composites of polycaprolactone (PCL) and vital wheat gluten (VG) were extruded, injection-molded, and analyzed using differential scanning calorimetry (DSC), thermogravimetric analysis (TGA), scanning electron microscope, and Fourier-transform infrared (FTIR). Neat PCL sample was cooled down to -70°C and heated to 150°C , where a glass transition (T_g) emerged at -67.0°C [$0.20\text{ J}/(\text{g }^{\circ}\text{C})$] followed by a melting transition at 56.6°C . At the end of the heating cycle, a cooling cycle started, where the same sample exhibited crystallization transition at 30.1°C . VG exhibited a T_g at 63.0°C [$0.45\text{ J}/(\text{g }^{\circ}\text{C})$]. Data analysis of TGA showed a one-step degradation mechanism of neat PCL versus multiple steps for the composites, indicating similar molecular structure and physical properties of neat PCL unlike the compo-

sites. In nitrogen environment versus air, the degradation activation energy (E_a) of the composites has increased at higher VG levels. From the DSC and TGA data, it is apparent that some physical interaction between PCL and VG was present. The FTIR analysis verified the physical nature of this interaction as opposed to chemical interaction. Proteinase degradation activity on the extruded composites was much higher than the injection-molded as indicated by higher weight loss in the extruded samples. © 2008 Wiley Periodicals, Inc. *J Appl Polym Sci* 110: 3256–3266, 2008

Key words: extruded; injection-molded; DSC; TGA; crystallinity; gluten; PCL; degradation mechanism; SEM; surface energy; FTIR; proteinase-K

INTRODUCTION

Despite the convenience and the practicality of the petroleum-based polymers used for food and other consumer goods packing, there is evidence for ecological disturbance. There is ongoing appeal and need for developing new uses for agricultural byproducts for environmental protection such as biodegradable plastics. The development and use of biodegradable plastics in packaging for environmental protection have been stimulated by the public concerns and interest, especially food packaging, the biggest users of packaging material. The thermomechanical properties of these products, however, need

to be examined by the food industry for any possible incompatibility with certain foods or storage conditions. Cao et al. reported a promising blend of poly(lactic acid) (PLA) and poly(hydroxy ester ether) (PHEE) and cornstarch as a promising blend.¹ PHEE polymer is an amorphous thermoplastic material used for its good adhesion properties with glass transition at 45°C .^{2–4} Cao et al. also reported higher intrahydrogen bonding at 50% PLA level in the PHEE composite as shown by solid-state Fourier-transform infrared (FTIR) spectroscopy. At 60% PLA and higher, the carbonyl groups of PLA and hydroxyl groups of PHEE started forming interhydrogen bonding. In a previous work, starch-PLA composites were prepared by extrusion and the two polymers were found immiscible. The presence of starch did not change the thermal properties of PLA in these composites, whereas the crystallinity, the tensile strength, and elongation of the composite has decreased at higher starch content.^{5,6} Another composite was prepared, by extrusion, from modified polycaprolactone resin (PCL), soy protein, and polyesters. PCL was modified by adding a maleic anhydride group to act as a compatibilizer.^{7,8} Jacob et al.⁷

*The USDA neither guarantees nor warrants the standard of the product, and the use of the name by the USDA implies no approval of the product to the exclusion of others that may also be suitable.

Correspondence to: A. Mohamed (a.mohamed@ars.usda.gov).

Journal of Applied Polymer Science, Vol. 110, 3256–3266 (2008)
© 2008 Wiley Periodicals, Inc. *This article is a US Government work and, as such, is in the public domain in the United States of America.

reported a PCL-gluten composite containing up to 75% (W/W) gluten without significant change in the tensile properties of PCL; however, the elongation has decreased and both G' and G'' were a magnitude higher than the neat PCL.

The objectives of this work were to compose blends by using commercial PCL and wheat gluten. Gluten was used as a filler, whereas PCL as a continuous phase because of its semicrystalline structure. The use of wheat gluten, a byproduct of the wheat-starch industry, will indirectly increase profitability of the industry. This is consistent with our effort to develop new uses for agricultural commodities or their byproducts and to further support the effort to protect the environment. This article is focused on the thermal properties of PCL/wheat gluten blends using differential scanning calorimetry (DSC) and thermogravimetric analysis (TGA), and another publication will deal with the mechanical properties.

EXPERIMENTAL

Materials and polymer blend preparation

PCL and vital gluten were obtained from commercial sources and were used as received. PCL was obtained from Dow Chemical (Midland, MI) (trade name: Tone 787) and vital gluten (VG) was provided by Midwest Grain Company (Pekin, IL). Binary blends of PCL with vital gluten were prepared by manually mixing the corresponding PCL pellet and VG powder. The blends composition ranged from 100% pure (neat) PCL to 30%, in 10% (w/w) intervals; 90 : 10, 80 : 20, 70 : 30, 60 : 40, 50 : 50, and 30 : 70.

Extrusion processing and injection molding

PCL-VG composites were compounded using a Werner-Pfleiderer ZSK30 corotating twin-screw extruder (Coperion, Ramsey, NJ). The barrel comprised 14-barrel sections giving a length/diameter ratio of 44 : 1, and the screw speed was 150 RPM. PCL was fed into barrel section 1 using a gravimetric feeder (Model 3000, AccuRate, Whitewater, WI). After melting PCL, wheat gluten was fed into barrel section 7 using a loss-in-weight feeder. The barrel was heated using eight heating zones. The temperature profile was 88°C (Zone 1) and 127°C (Zones 2–8). A die plate with two holes (4-mm diameter) was used. The melt temperature of the extrudate at the die was ~ 100°C for neat PCL and increased to 120°C with increasing gluten content. Residence time was ~ 2.5 min. Die pressure, torque, and feed rate were allowed to stabilize between formulations before the sample was collected. Strands were pelletized using

a Laboratory Pelletizer (Killion Extruders, Cedar Grove, NJ).

An ACT75B injection molder (Cincinnati Milacron, Batavia, OH) was used to injection mold ASTM D 638-99 Type I tensile bars (Master Precision Mold, Greenville, MI). Preventive measures were taken to assure that the surfaces of the composites were not contaminated. For increased gluten level, the barrel temperatures had to be adjusted upward and cooling time increased to help forward material while still cooling the feed section. Packing pressures were inverted for samples due to extreme flashing characteristics. Because of the decreasing density of the feeds, pressure was applied to the feed throat to help forward material. The cooling time was 35–45 s, the maximum injection pressure was 14,000 PSI, and the mold temperature was 45°C.

Differential scanning calorimetry

DSC measurements were carried out using a DSCTM Q2000 (TA Instruments, New Castle, DE). At first, composites were ground into powder using a Brinkmann/Retsch high-speed shaker mill. Powdered sample (~ 50 mg) was loaded and sealed in a stainless steel high volume pan. Samples were equilibrated for 1.0 min in the DSC at 0°C after which the temperature has increased to 200°C at 10°C/min, isotherm was maintained for 1 min, and the sample was cooled to -70°C at the same rate. The DSC data include glass transition (T_g), melting, and crystallization transitions parameters, such as onset or peak temperatures and ΔH .

Thermogravimetric analysis

TGA measurements were taken using a TGA 2920 Thermogravimetric Analyzer (TA Instruments, New Castle, DE). Samples (~ 10 mg powder) were heated from room temperature to 800°C at 10°C/min and held at an isotherm for 3 min. The TGA data were plotted as temperature versus weight percent, from which onset and final decomposition temperatures were obtained. Hereafter, these plots will be referred to as TGA plots. The TGA data were also plotted as temperature versus derivative of weight percent, from which the peak decomposition temperatures were obtained (these plots will be referred to as DTGA plots.).

Additionally, TGA data were used to determine the degradation kinetics of neat PCL or composites. Three heating rates, 10, 15, 20°C/min, were used to calculate the activation energy of degradation (E_a) according to Flynn and Walls⁹ based on the following eq. (1):

$$\log \beta \cong 0.457 \left(-\frac{E_a}{RT} \right) + \left[\log \left(\frac{AE_a}{R} \right) - \log F(a) - 2.315 \right] \quad (1)$$

where β is the heating rate, T is the absolute temperature, R is the gas constant, a is the conversion, E_a is the activation energy, and A is the pre-exponential factor. According to this equation, E_a can be obtained from the slope of the plot of $\log \beta$ versus $1000/T$ (K) at the same percent conversion. The E_a was calculated using the software provided by the TGA manufacture (TA Instruments), where the E_a value was determined for all samples at each heating rate and percent conversion.

Enzymatic degradation and SEM

Composites (EX or IM) were cut to pieces with similar dimensions (10 mm wide \times 10 mm long \times 3.5 mm thickness).¹⁰ Enzyme buffer, 0.05M Tris-HCl pH 8.6, was prepared (dissolved 0.91 g Tris in 150 mL Millipore water and adjusted to 8.6 using 1N HCl). Proteinase-K enzyme (60 mg contain 7.5 U/mg solid) and 30 mg sodium azide were added to 150 mL buffer. Each sample (4 pieces) was immersed in 5 mL of enzyme buffer and stored at 37°C with occasional shaking. After 24 h, the enzyme solution of each sample was replaced with fresh buffer to maintain maximum enzymatic activity. After 72 h storage, samples were rinsed with distilled water and dried under vacuum for 24 h. The difference in weight before and after enzyme treatment was recorded and the percent weight loss was calculated. Dried samples were mounted onto aluminum specimen holders, using silver paint (Fullman, Latham, NY) samples were coated under vacuum with gold-palladium at 200/min in a BLANK sputter coating unit. The samples were then photographed in scanning electron microscope (JEOL JXM 6400, JEOL, Tokyo, Japan) at 10 kV.

Fourier-transform infrared spectroscopy

Before FTIR spectroscopy analysis, samples were pulverized cryogenically in liquid nitrogen (-70°C) to minimize the particle size of the powders while preserving the primary and secondary molecular structures of the polymers. Cryogenic pulverization produced clear KBr pellets with transparency approaching that of solid solutions.¹ Also, it minimized absorption of water vapor from the atmosphere by KBr during pulverization and thereby prevented spectral interference from water bands in the important amide I region in gluten and the ester region in PCL. The powders were tested after drying under vacuum at 30°C for 24 h to eliminate water

vapor. The test samples were pressed into KBr powder to give disc-shaped pellets (13 mm \times 1 mm).

FTIR spectra were measured on an FTS 6000 spectrometer (Varian, Walnut Creek, CA) equipped with a DTGS detector. The absorbance spectrum (4000–400 cm^{-1}) for each sample was acquired at 4 cm^{-1} resolution and signal-averaged over 32 scans. Interferograms were Fourier-transformed using triangular apodization for optimum linear response. Spectra with corrected baseline, scaled to adjust for differences in sample weights, and normalized to selected peak heights for comparison, were presented.

Surface energy analysis

The contact angle of diiodomethane and deionized water were measured as a function of wheat gluten concentration using Geometric Mean method. The procedure and the apparatus used for contact angle measurements are detailed in a previous publication.¹¹ The total surface energy of the samples (γ_{st}), polar (γ_{sp}), and dispersive (γ_{ds}) components was estimated using wettability method.

Statistical design

A completely random design (CRD) was used in a General Linear Model approach for modeling thermal properties as a function of % gluten for two methods. Regression equations were developed for six thermal property Y -variables (Melt Onset T , Melt Peak T , Melt ΔH , Crystal Onset T , Crystal Peak T , and Crystal ΔH) as a function of % gluten (0, 10, 20, 30, 40, 50, and 70%) for two methods (extrusion and injection). Gluten levels within a method were compared and the methods were compared at each gluten level using 95% confidence intervals on predicted values of the thermal property variables from the equations. If the confidence intervals for predicted values overlap, then no significant differences exist. All analyses were performed using TableCurve 2D v5.00, AISN Software, 2000.

RESULTS AND DISCUSSION

Differential scanning calorimetry

Polymer composites characteristics can be predicted based on DSC measurements that include degree of miscibility, degree of intermolecular interactions, and degree of crystallization.^{12–16} For instance, the general rules for evaluating miscibility of binary blends using DSC are along these lines: (a) immiscible—a blend which displays two T_g and two T_m that are considered composition-independent; (b) miscible—a blend that displays composition-dependency indicated by a single T_g and a single T_m in the entire

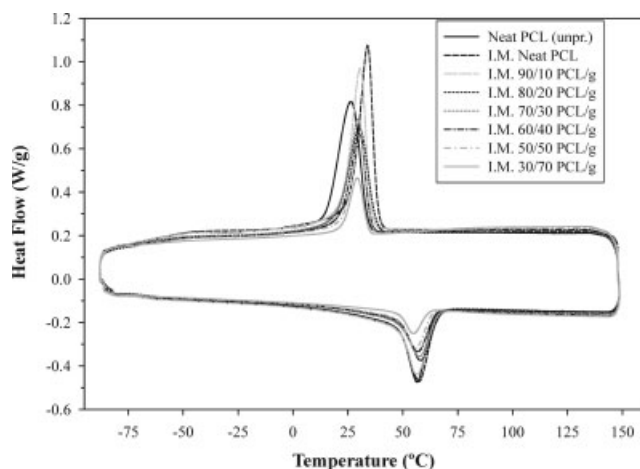


Figure 1 Heating and cooling DSC profiles of injection-molded PCL/vital gluten composites at different vital gluten levels.

composition range; (c) partially miscible—a blend that displays two T_g and two T_m that are composition-dependent¹⁶ and/or composition-dependent single T_g and single T_m in a narrow composition range. The DSC profiles of the neat PCL and PCL composites are shown in Figure 1. To eliminate the thermal history of PCL, all DSC data discussed later and shown in Figure 1, represent the second heating and cooling DSC cycles. Each PCL cycle included a glass transition (T_g), endothermic during heating (melting), and exothermic during cooling (crystallization) transitions, whereas vital gluten (VG) exhibited only glass transition (T_g). The corresponding heat capacity (ΔC_p) and T_g temperatures obtained from the DSC data of the neat polymers and composites are given in Table I. The T_g temperature of neat PCL and VG are -67.8°C and 63.0°C , respectively, whereas the ΔC_p exhibited 0.21 and $0.45 \text{ J}/(\text{g } ^\circ\text{C})$. It is important to mention the presence of one T_g for the composite, which is one of the indications of miscibility or interaction. The T_g temperature of the composites, as shown in Table I, is much closer to that of PCL as apposed to VG. The nature of the

interaction seemed to be physical rather than chemical (possibly hydrogen bonding), as it will be shown in the FTIR data discussion. The T_g temperature of the composite appeared to be independent from the amount of VG in the composite, which indicates the absence of chemical interaction between PCL and VG during extrusion and injection-molding. The ΔC_p values of the composites continued to stay around the ΔC_p of PCL (0.21) and not the VG [$0.45 \text{ J}/(\text{g } ^\circ\text{C})$]. This trend and the trend of T_g temperature indicate the domination of PCL molecular mobility over VG. The presence of one T_g in the composites profiles around PCL value reflects molecular mobility closer to neat PCL.

The regression equations used for predicting the effect of different VG levels on PCL onset or peak temperatures and ΔH (parameters) are shown in Table II. The equations were then used to determine if any parameter was significantly different within the extruded samples (column) and between extruded and injection-molded samples (Tables III and IV). The increase in VG content significantly reduced the onset in the melting and the cooling cycles of the extruded and injection-molded samples, whereas the comparison between extruded and injection-molded revealed significant differences only during the cooling cycle. The peak temperatures of both melting and cooling within extruded and within injection-molded exhibited similar trend as onset, whereas ΔH showed significantly higher values only during the melting cycle (Tables III and IV). Higher melting temperature signifies some sort of interaction between VG and PCL. The effect of VG was obvious on the ΔH values for both DSC cycles, where ΔH (J/g) was dropped according to the added VG percentage, i.e., 10% VG added reduced the ΔH by 10%.

A number of mathematical models were used for predicting T_g temperature dependence of polymer composites, such as Gordon-Taylor-Woods eq. (2).¹⁷

$$T_{g1}^b = \frac{W_1 T_{g1} + K W_2 T_{g2}}{W_1 + K W_2} \quad (2)$$

TABLE I
Summary of Differential Scanning Calorimetry Analysis of Neat PCL, Vital Gluten, and PCL/Vital Gluten Composites

		PCL	30/70	50/50	60/40	70/30	80/20	90/10	VG ^a
EX ^b	T_g^c ($^\circ\text{C}$)	-67.5	-68.50	-67.85	-67.6	-67.75	-67.80	-67.90	63.00
	ΔC_p^d	0.20	0.09	0.13	0.15	0.18	0.19	0.19	0.45
IM ^e	T_g ($^\circ\text{C}$)	-67.25	-69.45	-67.75	-67.5	-67.50	-67.10	-68.10	63.80
	ΔC_p	0.19	0.10	0.13	0.14	0.17	0.18	0.19	0.46

^a VG, vital gluten.

^b EX, extruded.

^c T_g , glass transition.

^d ΔC_p in $\text{J}/(\text{g } ^\circ\text{C})$.

^e IM, injection-molded.

TABLE II
Regression Equations of Thermal Properties Variables as a Function of Percent Vital
Gluten for the Extruded and Injection-Molded Composites

Thermal property	Regression equation	Adj. ^a R ^b
Endo ^c onset EX	$Y = 48.01 - 0.13X + 0.012X^{1.5}$	0.98*
Endo onset IM	$Y = 47.8 - 0.02X^2 + 0.005X^{2.5} - 0.0003X^3$	0.80
Endo peak EX	$Y = 56.59 + 0.47X - 0.04X^{1.5} - 1.16X^{0.5}$	0.82
Endo peak IM	$Y = 57.55 - 0.0006X^2$	0.87*
Endo ΔH EX	$Y = 77.83 - 0.69X$	0.97*
Endo ΔH IM	$Y = 77.28 - 0.73X$	0.998*
Exo ^b onset EX	$Y = 34.36 - 0.57X + 0.15X^{1.5} - 0.012X^2$	0.996*
Exo onset IM	$Y = 37.61 - 0.69X + 0.17X^{1.5} - 0.011X^2$	0.91
Exo peak EX	$Y = 30.33 - 0.67X + 0.16X^{1.5} - 0.012X^2$	0.95**
Exo peak IM	$Y = 33.21 - 0.9X + 0.22X^{1.5} - 0.014X^2$	0.98*
Exo ΔH EX	$Y = 102.54 - 0.99X$	0.997*
Exo ΔH IM	$Y = 98.19 - 0.91X$	0.999*

^a Adjusted R² values show the amount of variability in the data explained by the equation.

^b Exo, exothermic transition.

^c Endo, endothermic transition.

All regression coefficients are significant at $P \leq 0.05$.

* Equations significant at $P \leq 0.01$.

** Equations significant at $P \leq 0.05$.

TABLE III
Endothermic Transition Confidence Interval Comparison
of Percent Gluten at the 95% Level Within Each Method
for Each Thermal Property Variable and Between
Methods for Each Thermal Property

Thermal property	Gluten (%)	Predicted Y and 95% CI	
		Extruded	Injection-molded
Melting onset (°C)	0	48.01 (a) ^a	47.80 (a)
	10	47.14 (b)	47.07 (ac)
	20	46.58 (c)	46.24 (bcd)
	30	46.23 (d)	45.96 (d)
	40	46.05 (d)	46.23 (cd)
	50	46.01 (d)	46.76 (a-d)
Melting peak (°C)	70	46.31 (c)	46.52 (a-d)
	0	56.59 (abc)	57.55 (a)
	10	56.26 (b)	57.49 (ab) ^b
	20	56.95 (a)	57.32 (ab)
	30	57.25 (a)	57.03 (ab)
	40	57.14 (ab)	56.63 (bc)
Melting ΔH (J/g)	50	56.63 (ab)	56.11 (c)
	70	54.50 (c)	54.74 (d)
	0	77.83 (a)	77.28 (a)
	10	70.91 (a)	69.98 (b)
	20	63.99 (b)	62.68 (c)
	30	50.15 (c)	55.38 (d) ^b
	40	43.24 (d)	48.08 (e) ^b
	50	29.40 (e)	40.78 (f) ^b
	70	77.83 (a)	26.18 (g)

^a Predicted Y-values within a thermal property and method followed by different lowercase letters indicate significant differences between Gluten levels based on nonoverlap of the 95% confidence intervals from the regression equations.

^b Predicted Y-values within a thermal property and gluten level indicate significant differences between methods based on nonoverlap of the 95% confidence intervals from the regression equations.

TABLE IV
Exothermic Transition Confidence Interval Comparison
of Percent Gluten at the 95% Level Within Each Method
for Each Thermal Property Variable and Between
Methods for Each Thermal Property

Thermal property	Gluten (%)	Predicted Y and 95% CI	
		Extruded	Injection-molded
Cooling onset (°C)	0	34.36 (ab) ^a	37.61 (a) ^b
	10	32.33 (e)	34.93 (bc) ^b
	20	32.28 (e)	34.46 (c) ^b
	30	32.87 (d)	34.68 (c) ^b
	40	33.63 (c)	35.05 (bc) ^b
	50	34.28 (b)	35.26 (b) ^b
	70	34.55 (a)	34.39 (c)
Cooling peak (°C)	0	30.33 (a)	33.21 (a) ^b
	10	27.72 (de)	29.72 (cd) ^b
	20	27.35 (e)	29.13 (d) ^b
	30	27.76 (de)	29.47 (d) ^b
	40	28.43 (cd)	30.01 (c) ^b
	50	29.05 (bc)	30.34 (b) ^b
	70	29.42 (ab)	29.36 (d)
Cooling ΔH (J/g)	0	102.50 (a)	98.19 (a)
	10	92.68 (b)	89.13 (b)
	20	82.82 (c)	80.07 (c)
	30	72.97 (d)	71.00 (d)
	40	63.11 (e)	61.94 (e)
	50	53.26 (f)	52.88 (f)
	70	33.55 (g)	34.75 (g)

^a Predicted Y-values within a thermal property and method followed by different lowercase letters indicate significant differences between gluten levels based on nonoverlap of the 95% confidence intervals from the regression equations.

^b Predicted Y-values within a thermal property and gluten level indicate significant differences between methods based on nonoverlap of the 95% confidence intervals from the regression equations.

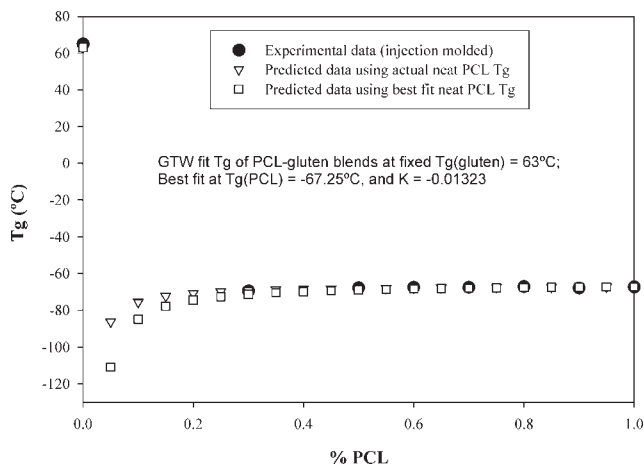


Figure 2 Experimental and predicted glass transition (T_g) values based on actual and best-fit T_g of PCL according to Gordon-Taylor-Wood equation.

where T_g^b = composite glass transition, W_1 and W_2 = weight fraction of PCL and VG, respectively, T_{g1} and T_{g2} = glass transition of PCL and VG, respectively, and K = adjustable fitting parameter related to miscibility, i.e., the strength of the physical or chemical interaction between PCL and VG. The K value is unique for each blend. Equation (3) is the linear form of the Gordon-Taylor equation, where K is the slope of the straight line.

$$T_g^b = T_{g1} + K \left[\frac{W_2}{W_1} (T_{g2} - T_g^v) \right] \quad (3)$$

where $\frac{W_2}{W_1} (T_{g2} - T_g^b) = X$, and $T_g^b = Y$, and $K = \text{slope}$.

The value of the parameter K in eq. (3) cannot be used for completely different blend ratios.¹⁸ Gordon-Taylor-Wood is a modified form of Gordon-Taylor equation, where T_g of one of the components of the composite is fixed and the T_g of the other component was varied to attain the best fit. The Gordon-Taylor-Woods eq. (4) is as follows:

$$T_g^b = \frac{W_1 T_{g1} + K(1 - W_1) T_{g2}}{W_1 + K(1 - W_1)} \quad (4)$$

T_g^b = T_g of the composite; W_1 is % VG in blend; $T_{g1} = T_{gPCL}$, $T_{g2} = T_{gVG}$; T_{gVG} was fixed at 63°C; K and T_{gVG} were used as fitting parameters.

$$T_g^b = \frac{\{T_{gPCL} \times [\text{PCL}] + K \times T_{gVG} \times (1 - [\text{PCL}])\}}{\{[\text{PCL}] + k \times (1 - [\text{PCL}])\}} \quad (5)$$

Best fit was obtained at $T_{gPCL} = -67.25^\circ\text{C}$ (close to measured value of -64.0°C in Table I) and $k = -0.01323$. Three sets of data are represented in Figure 2, and PCL/VG blends were determined using eq. (5). The three lines in Figure 2 represent the predicted T_g temperature at a fixed 63.0°C for VG, the

predicted T_g using PCL's T_g value with the best fit (-67.25°C) for the Gordon-Taylor-Woods equation, and finally the line based on the seven experimental data points used for the equation fitting. The profiles represented in Figure 2 signify the similarity between the Gordon-Taylor-Wood prediction and the analytical data based on the seven experimental data points. This fitting is specific for the $K = -0.01323$.

Thermogravimetric analysis

Neat PCL showed a simple (one-step) decomposition profile with a single transition temperature, as

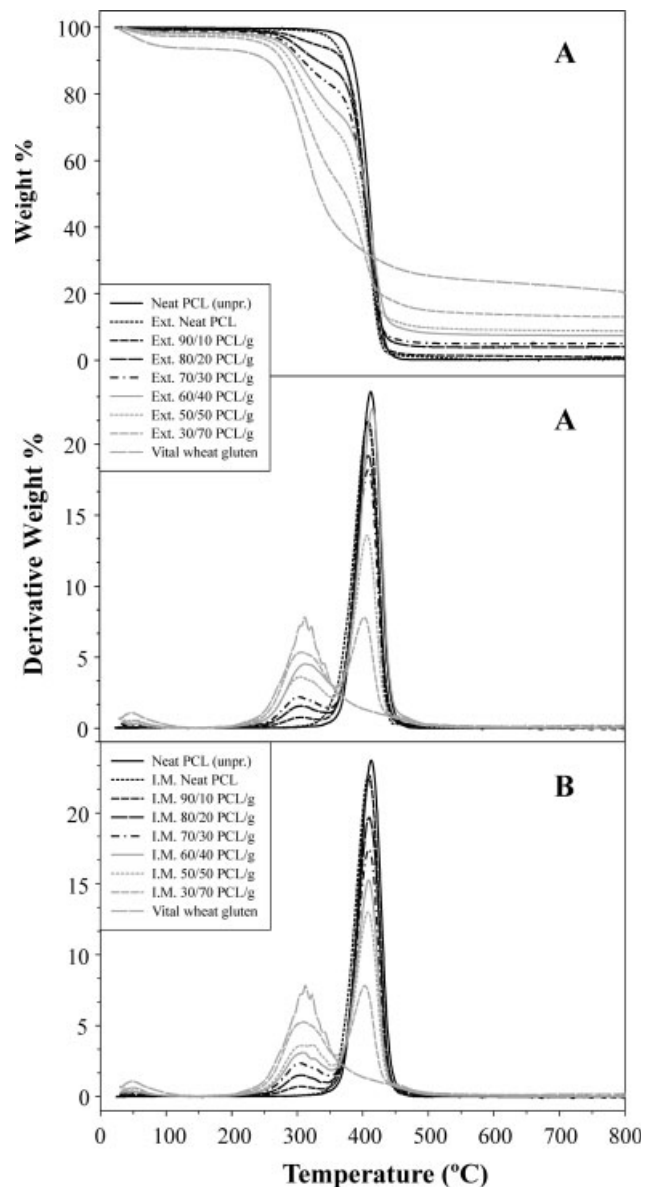


Figure 3 (A) Thermogravimetric (TGA) profiles of extruded PCL/vital gluten composites including the DTGA profile. (B) Derivative thermogravimetric (DTGA) profiles of injection-molded PCL/vital gluten composites.

TABLE V
Thermogravimetric Onset, Peak, and Final Temperatures and the Residues at Each Temperature for Neat Polymers and Composites

Sample	Profile no. 1			Profile no. 2		Final	
	Onset (°C)	Peak (°C)	Residue (%)	Peak (°C)	Residue (%)	Temperature (°C)	Residue (%)
VG	211			Neat polymer		649	20.4
30/70	209	324	72	412	34	603	14.7
50/50	213	322	82	418	35	535	9.43
60/40	217	310	93	420	40	517	9.47
70/30	227	313	92	420	38	508	4.86
80/20	228	316	94	420	40	494	3.91
90/10	219	316	97	421	43	512	1.37
PCL	342			Neat polymer		489	0.35

demonstrated by TGA and the derivative plots (DTGA) [Fig. 3(A,B)]. The neat-PCL degradation profile showed higher thermal stability than VG, because it started degrading at 342°C and completely decomposed (0% w/w char residue) at 489°C, whereas VG started degrading at 211°C and was not fully degraded after 800°C. Figure 3 profiles signified the effect of each polymer on the degradation mechanism of the composites. It is clear from the profile in Figure 3 that the presence of two steps degradation reflected the two polymers in the composite [Fig. 3(B)]. In addition, the profile-shape exemplified a common degradation temperature for both polymers, i.e., initially gluten started degrading and before it was fully degraded, PCL started degrading. Although the degradation profiles of neat PCL and VG are clear when looked at individually, the composite showed no clear distinction between the two polymers, i.e., the degradation profile showed a gradual weight loss rather than a sharp drop on the weight loss. A good example of a sharp drop in weight loss can be seen in the TGA analysis of PCL/PS composite.¹⁹ This gradual drop in weight could indicate the presence of a material resulting from blending these two polymers that contains different properties. This data is in line with the DSC data, where the composites exhibited only one glass transition. It is worth mentioning that biomaterials, including VG, fully decompose in air environment at 600°C for 2 h, as apposed to nitrogen [Fig. 3(A,B)]. At any given temperature, composites showed different degradation rates as indicated by the different amounts of residue (Table V). It is noticeable in Table V that the influence of VG on the onset temperature of the composites ranged between 211 and 219°C, whereas PCL impacted the peak temperatures of the composites which ranged between 324 and 316°C. The residues of the neat polymers or the composites are listed in Table V, where a single residue was listed for each neat polymer. There were three residues with different values listed from each composite. The amounts of these residues var-

ied for each composite according to composition as expected. As listed in Table V, a higher residue value is an end result of higher VG content. The important thing to notice is the variation in the range between the highest and the lowest residue for each profile (Table V). The first profile showed that the percentage difference between the highest and the lowest residue was 25%, the second profile was 9%, and the third was 13.3%. This could be considered as an indication of the different degradation mechanism of these composites.

Degradation kinetics

The calculation of the activation energy (E_a) of degradation using the data collected from TGA is derived from three equations.

$$R = \frac{da}{dt} = K(T)f(a) \quad (6)$$

where $f(a)$ is the reaction model, a is the extend of the reaction, $K(T)$ is the temperature-dependent rate constant, " T " is the temperature, " t " is the time, and R is the degradation rate. It is assumed that the term $K(T)$ obeyed Arrhenius law as follows:

$$K(T) = A \exp\left(\frac{-E_a}{RT}\right) \quad (7)$$

where A is the pre-exponential factor, E_a is the activation energy, a is the conversion, and R is the gas constant. In addition, the degradation is considered as a simple n th-order reaction, which results in the following expression of the conversion-dependant:

$$f(a) = (1 - a)^n = W^n \quad (8)$$

where n is the reaction order and W is the weight of the remaining un-degraded material. The three methods are used for single heating rates analysis or multiple heating rates. By applying Doyle's¹⁶

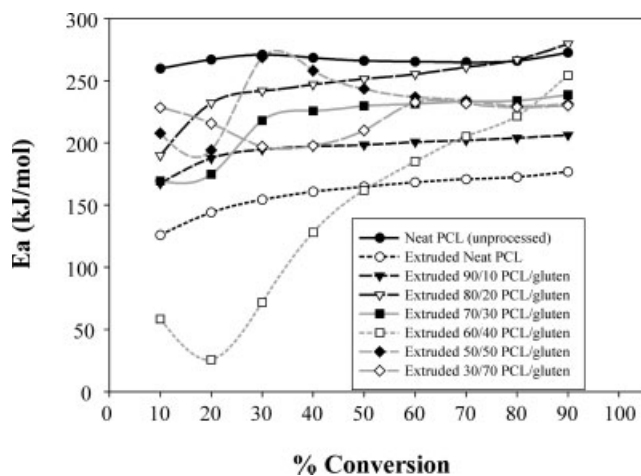


Figure 4 Decomposition kinetics profiles of extruded PCL/vital gluten composites.

approximation to the integrated form of eq. (6), we obtain the Flynn-Wall equation (1).⁹ The activation energy E_a can be obtained from the slope of the straight line plot of $\log \beta$ against $1000/T$ (K). The details of the calculation are reported in a previous publication,¹⁸ where the E_a was calculated using the software provided by the manufacturer of the TGA (TA Instruments). The degradation mechanism of the composites can be obtained by plotting the percent degradation conversion versus E_a as shown in Figures 4 and 5. The straight line resulting from steady increase on the E_a as the percent conversion increased signifies one-step degradation. The composites showed lines with varying E_a values as the percent conversion increased. This phenomenon is similar to the trend noticed in Table V, where the residue each profile of all composites were different. Neither TGA nor DSC is the best method to deter-

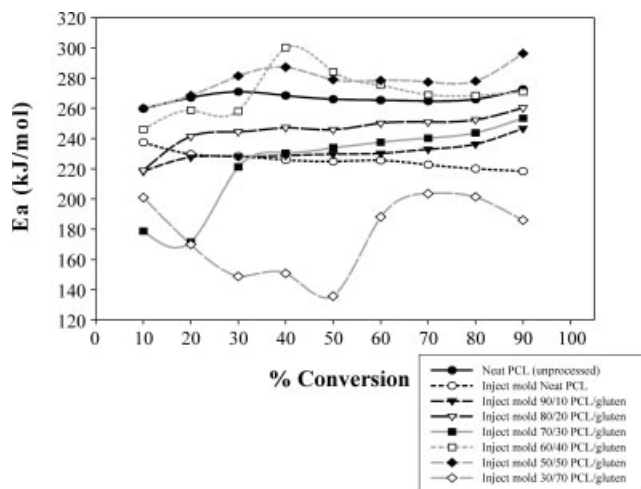


Figure 5 Decomposition kinetics profiles of injection-molded PCL/vital gluten composites.

mine the type of interaction between the components of these composites, but these methods are good indicators of interaction. The E_a of the extruded (EX), injection-molded (IM), unprocessed (UP), and neat PCL (N) exhibited a one-step degradation mechanisms (Figs. 4 and 5). Therefore, neat PCL degradation was not influenced by processing. Despite the one-step degradation of neat PCL, E_a value of $N > IM > EX$ signifying the effect of processing on the E_a value of neat PCL and not the mechanism. The composites showed a mixed mechanisms with more than one-step degradation, where 60/40 composite showing the lowest E_a and the most complicated mechanism (Figs. 4 and 5). To examine the effect of gluten on the E_a of the composites, the %VG was also plotted against E_a at the 50% degradation conversion. The E_a of the composites has increased gradually as a function of %VG (Fig. 6) for up to 50% gluten content except at 60/40, where E_a exhibited the lowest value. The same composite (60/40) had the most abnormal degradation mechanism as well (Figs. 4 and 5). At 70% VG, the E_a dropped significantly for the injection-molded composites, whereas the extruded stayed above the neat PCL value. Figure 6 as well as FTIR point to some kind of interaction (physical) between the PCL and VG. The significant increase in degradation E_a could also be caused by the slow degradation of VG in nitrogen environment.

Enzymatic degradation and scanning electron microscope

The enzymatic degradation of the composite is dependant on the processing method (EX or IM) and VG content. Higher amounts of VG increased the weight loss following enzyme treatment (Fig. 7). Neat

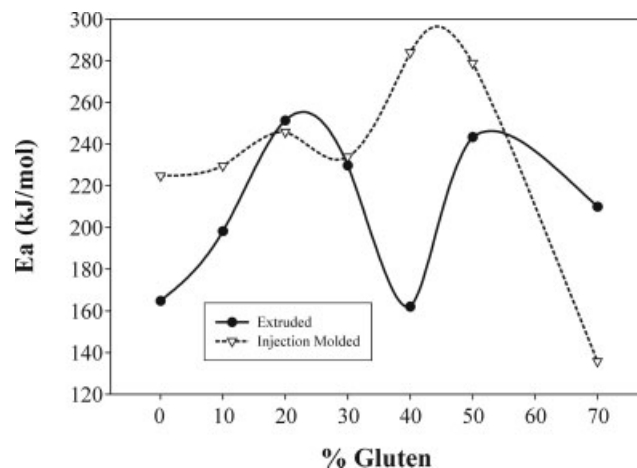
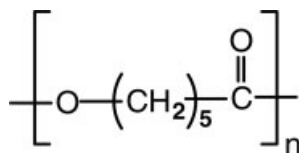


Figure 6 Decomposition activation energy (E_a) of extruded and injection-molded PCL/vital gluten composites.

PCL (EX or IM) exhibited minimal weight loss after enzymatic degradation, whereas higher VG content steadily increased composites weight-loss signifying higher enzymatic activity as a function of %VG. The compact nature of the IM samples reduced the enzymatic attack when compared with the loose structure of the extruded composites (Fig. 7). The compactness of the IM composites was also related to the significantly higher ΔH as shown in Table III. The slow degradation rate of the IM samples can be observed on the SEM images (Fig. 8). In the presence of less VG, the image of the EX composite was discontinuous, whereas IM appeared more compact. The SEM images of the 50% VG versus 30% composites showed how gluten is forming continuous mass. The darker color of the IM 50% VG when compared with the 30% was due to browning reaction between proteins and carbohydrates at elevated processing temperature during injection-molding.

Fourier-transform infrared spectroscopy

Figure 9 shows the FTIR spectra of PCL and gluten overlaid.



The spectrum of PCL shows a strong carbonyl ($\text{C}=\text{O}$) peak at 1729 cm^{-1} and medium peaks between 2868 and 2949 cm^{-1} from methylene (CH_2) groups in PCL. Since gluten is a protein, its characteristic infrared spectral features arise from amino acid structural groups such as those in the tripeptide chain of alanine, cysteine, and serine,

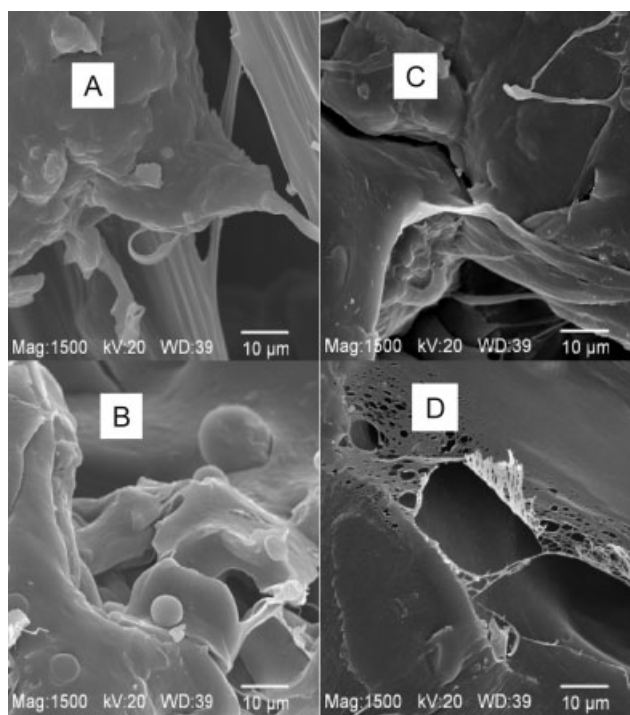
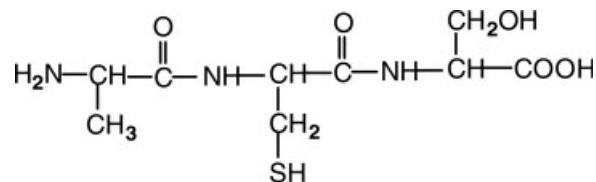


Figure 8 Scanning electron microscope images of PCL/vital gluten composites. EX, extruded; IM, injection-molded.



However, the sequences of the different amino acids in polypeptide chains of protein are thousands of times longer. Therefore, the spectrum of gluten in Figure 9 contains a strong amide I ($\text{C}=\text{O}$) peak at

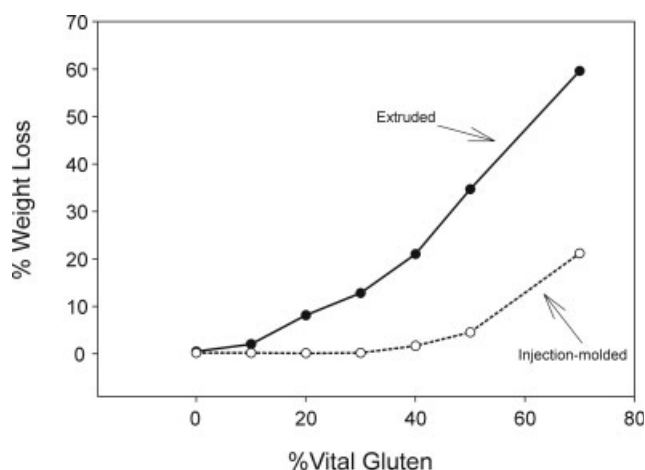


Figure 7 Effect of percent vital gluten on the enzymatic degradation of extruded and injection-molded composite.

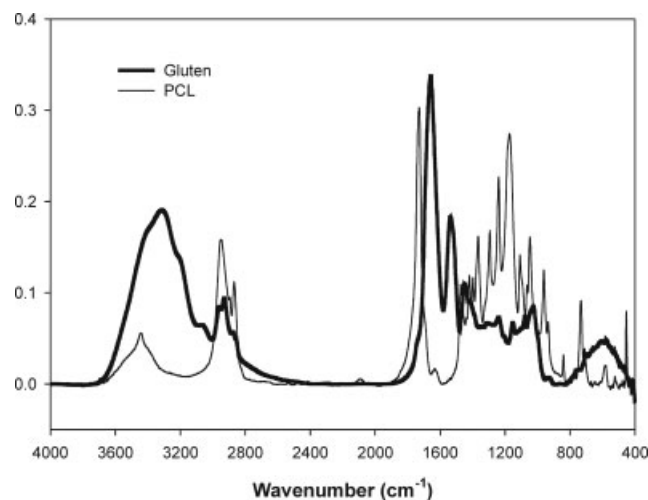


Figure 9 FTIR-PAS of neat PCL and gluten used as controls.

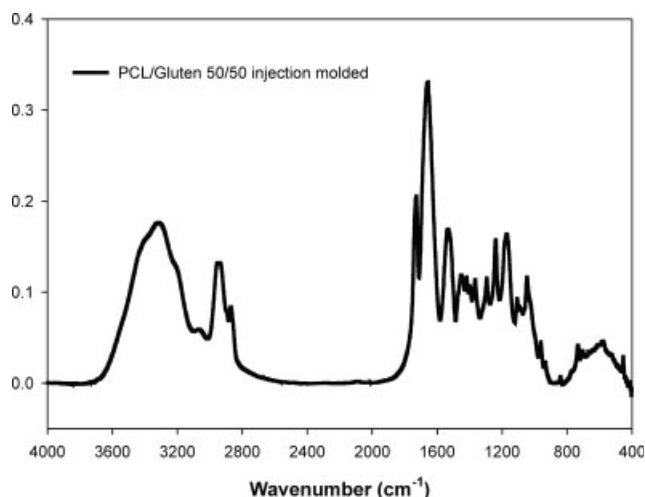


Figure 10 FTIR-PAS of 50/50 PCL:vital gluten injection-molded composite.

1640 cm^{-1} , a medium amide II (NH) peak at 1550 cm^{-1} , and broad hydroxyl (OH) bands centered at 3315 cm^{-1} , which are typical of proteins.

Solid-state FTIR spectroscopy of the unprocessed gluten and the extruded and injection-molded PCL/gluten mixtures revealed that no major chemical changes occurred in gluten or PCL during processing. In earlier work,²⁰ it was found that gluten underwent substantial deamination under heating at 190°C in a Brabender mixer. However, under the conditions of extrusion and injection molding used in this work, the chemical structure of gluten was not noticeably degraded. By comparison with the Brabender-treated gluten, the amide I (1640 cm^{-1}) and II (1550 cm^{-1}) peaks of the extruded and injection-molded gluten/PCL mixtures were not significantly decreased. Comparison of the FTIR spectra of neat (100%) PCL, processed and unprocessed, showed no chemical changes in PCL as well.

Examination of the carbonyl peak in PCL also revealed the absence of any appreciable molecular interaction of PCL with gluten in the processed mixtures. There was no measurable change or shift in the position of the carbonyl peak (1729 cm^{-1}) in any of the gluten/PCL mixtures after processing (Figs. 9 and 10). Therefore, from the FTIR spectra it is evident that the chemical structures of gluten and PCL (Fig. 10) were essentially preserved, and the simple physical mixture character of their blends was retained in extrusion or injection molding.

Surface energy analysis

Surface energy data (γ) is represented in Figure 11. The figure indicated that increasing the concentration of wheat gluten generally resulted in a slight decrease of the γ_{sp} (polar surface energy) value and a slight

increase in the γ_{ds} (dispersive surface energy) value of the composite. The overall result was a slight decrease in the γ_{st} (total surface energy) value of the composite with increasing wheat gluten concentration. The reported surface energy value for pure wheat gluten was 19.8–24.1, 29.4–32.9, and 52.7–53.5 (dyn/cm) for γ_{sp} , γ_{ds} , and γ_{st} , respectively,²¹ when compared with 0.3–10.3, 24.4–45.2, and 26.5–45.5 for pure PCL. The pure PCL analysis resulted from this work was 9.4, 45.3, and 54.6 (Dyn/cm). It was clear from the data sets that on the average, wheat gluten has a higher γ_{st} than PCL. It was also clear that wheat gluten has a higher polar surface energy component (γ_{sp}) than PCL. Based on the data sets presented earlier, one would expect that increasing the concentration of wheat gluten in the blend should result in higher γ_{sp} and γ_{st} values for the blend. However, as shown in Figure 11, these two values displayed the opposite effect, i.e., a slight decrease with increasing concentration of wheat gluten. This result implied that the concentration of PCL on the surface was higher than that in the blend. It appears that the blend component with the lower surface energy has disproportionately migrated to the surface. The consequence of this is an overall reduction of surface energy, which is the thermodynamically favored state for the composite. Such phenomenon are well known and widely observed in polymer blends comprising components that have significant differences in their surface energies.²²

CONCLUSIONS

Neat PCL showed higher heat degradation stability than vital gluten, whereas injection-molded samples exhibited higher enzymatic degradation stability. PCL had a T_g (−67.5°C) and a melting peak (56.9°C) during the heating cycle for, whereas VG is 100%

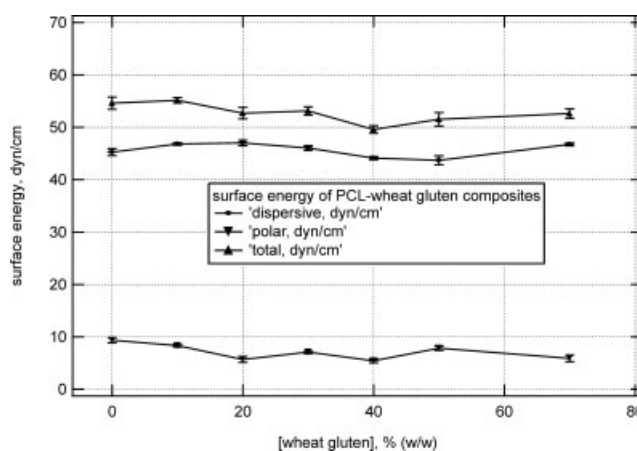


Figure 11 Surface energy of PCL/vital gluten composites obtained from the analysis of probe liquid contact angles using the geometric mean method (GM).

amorphous and exhibited a T_g at 63°C. The DSC analysis of the composites included one T_g closer to the T_g temperature of PCL indicating the absence of vital gluten T_g . Although, this is considered a strong indication of interaction between the two polymers, the FTIR-PAS analysis confirmed the existence of a physical interaction rather than chemical between PCL and vital gluten. The injection-molded samples analysis verified mostly the presence of PCL on the surface and not gluten as verified by surface energy determination and the SEM images.

The authors thank Jason Adkins for conducting the MDSC and TGA experiments; Ms. Danielle Wood for her help with the contact angle measurements. The authors also thank Richard Haig, Kathy Hornback, Gary Grose, and Brian Jasberg.

References

1. Cao, X.; Mohamed, A.; Gordon, S. H.; Willett, J. L.; Sessa, D. *Thermochim Acta* 2003, 406, 115.
2. Mang, M. N.; White, J. E. (Dow Chem Co., USA). *Eur. Pat. Appl.* (1992), 12 pp. CODEN: EXXDWP 513679 A2 19921119 Designate States R: BE, CH, ES, FR, GB, IT, LI, NL, SE. Patent written in English. Application: EP 92-107770 19920508. Priority: US 91-699046 199110513. CAN 118: 193009 AN 1993: 193009 CAPLUS [Copyright 2003 ACS on SciFinder (R)].
3. Mang, M.; White, J. Book of Abstracts, 210th ACS National Meeting, Chicago, IL, August 20–24, 1995.
4. Mang, M.; White, J. *Polym Mater Sci Eng* 1997, 76, 412.
5. Tianyi, K.; Xiuzhi, S. Physical properties of poly(lactic acid) and starch composites with various blending ratios. *Cereal Chem* 2000, 77, 761.
6. Jacobsen, S.; Fritz, H. G. *Polym Eng Sci* 1996, 36, 2799.
7. Jacob, J.; Jian, T.; Mrinal, B. *Polymer* 1998, 39, 2883.
8. Jacob, J.; Mrinal, B. *Polym Int* 1999, 48, 1165.
9. Flynn, J. H.; Wall, L. A. *Polym Lett* 1966, 4, 323.
10. Hua, C.; Vipul, D.; Gross, R. A.; McCarthy, S. P. *J Polym Sci* 1996, 34, 2701.
11. Mohamed, A.; Hojilla-Evangelista, M.; Peterson, S.; Biresaw, G. *J Am Oil Chem Soc* 2007, 84, 281.
12. Utracki, L. A. *Polymer Alloys and Blends*. Hansen: New York, 1990.
13. Krupa, I.; Luyt, A. S. *Polymer* 2001, 42, 7285.
14. Wong, A. C.-Y.; Lam, F. *Polym Test* 2002, 21, 691.
15. Mohamed, A.; Gordon, S. H.; Biresaw, G. *J Appl Polym Sci* 2007, 106, 1689.
16. Archondouli, P. S.; Kallitsis, J. K.; Kalfoglou, N. K. *J Appl Polym Sci* 2003, 88, 612.
17. Gordon, M.; Taylor, J. S. *J Appl Chem* 1952, 2, 493.
18. Painter, P. C.; Coleman, M. M.; Koenig, J. L. *The Theory of Vibrational Spectroscopy and Its Applications to Polymeric Materials*. Wiley-Interscience: New York, 1982.
19. Mohamed, A.; Gordon, S. H.; Biresaw, G. *Polym Degrad Stab* 2007, 92, 1177.
20. Mohamed, A.; Gordon, S. H.; Carriere, C. J.; Kim, S. *J Food Qual* 2006, 29, 266.
21. Blancher, G.; Morel, M. H.; Gastaldi, E.; Cuq, B. *Cereal Chem* 2005, 82, 158.
22. Biresaw, G.; Carrier, A. *J Polym Sci Part B: Polym Phys* 2001, 39, 920.